Observation of Mutually Trapped Multiband Optical Breathers in Waveguide Arrays

D. Mandelik,* H. S. Eisenberg,† and Y. Silberberg
Department of Physics of Complex Systems, the Weizmann Institute of Science, 76100 Rehovot, Israel

R. Morandotti‡ and J. S. Aitchison
Edward S. Rogers Sr. Department of Electrical and Computer Engineering, University of Toronto, Toronto, Ontario, Canada M5S 3G4

(Received 17 February 2003; published 25 June 2003)

Multiphoton fluorescence is used for the direct observation of a new class of breathers in waveguide arrays, which are a coherent superposition of Floquet-Bloch solitons of different bands. These Floquet-Bloch breathers oscillate along their spatial propagation axis, and possess several novel properties. Some behavior of these breathers is readily understood intuitively in terms of the band structure of the waveguide array and the properties of discrete solitons.

DOI: 10.1103/PhysRevLett.90.253902 PACS numbers: 42.25.Fx, 42.65.Wi, 42.65.Tg, 42.82.Et

The study of breathers has attracted growing attention in the past several years in a wide variety of physical (and biological) systems. These *intrinsic* localized excitations occur in perfectly regular systems (unlike the case of Anderson localization, for example, in which disorder drives the localization mechanism), when nonlinearity tunes the excitation's frequency into a gap in the linear spectrum of the system. Breathers are characterized by internal oscillations, in contrast with the well-studied solitons which maintain constant shape. Rigorous proof has been given for the existence of breathers [1], and their properties have been studied extensively [2,3]; however, their experimental observation has been reported only recently. Recent evidence points to the important role of breathers in an impressive variety of contexts, including low-dimensional materials [4], macroscopic-mechanical systems [5], spin lattices [6], spin waves in antiferromagnets [7], Josephson arrays [8] and Josephson ladders [9], molecular chains [10], Bose-Einstein condensates [11], dispersion managed optical fiber [12], and finally, optical breathers in photonic-crystal waveguides [13].

It is well known that two orthogonally polarized beams may be jointly trapped to form a spatial vector soliton [14,15]. Each of these beams by itself might not have enough power to support a soliton, and only when both beams are launched together (overlapping spatially), they mutually form a soliton. This concept has been extended to include other possibilities of two beams interacting incoherently to form a composite soliton [14,15]. In particular, numerical study of vector solitons in waveguide arrays has been recently reported [16], where each of the two beams is shaped such that it excites a particular Floquet-Bloch (FB) band of the waveguide array [17]. A self-consistency method was used to show that the two beams belonging to different bands are jointly trapped in the array to form a *multiband vector soliton*, propagating along the array without changing its envelope shape, assuming, again, that the two beams are mutually incoherent.

In this work, we report the observation of a new class of breathers in waveguide arrays, forming a coherent vector (or composite) soliton. These spatially localized breathers oscillate along their propagation axis and several of their properties may be understood intuitively in terms of the band structure of the waveguide array [17] and the properties of discrete solitons.

Consider the situation when light is injected into two FB bands of a waveguide array. The two beams interfere and form a complex pattern of intensity along the propagation direction. Figure 1 shows simulation results, using the beam-propagation method (BPM) [18], where light propagates in two FB bands (band No. 1 and band No. 2), which we relate to in the following as "FB beams"; Fig. 1(b) shows the two FB beams, when launched separately into the array at a power, which is not high enough to form a soliton (yet high enough to slow diffraction). The beams diffract in the array as FB waves, whose modal shapes are shown (enlarged) in the upper panel of the figure. In Fig. 1(c), the same beams (at the same power) are launched together into the array. The beams are shown to jointly trap one another, forming a breather, which propagates along the array. Such breathers were simulated for very long propagation distances, and within a range of parameters, proved to be stable. The breather may be understood intuitively in terms of the interference of the two FB beams, trapping each other into a nonlinear localized excitation, and propagating along the array at slightly different propagation constants, thereby beating and forming a breather. Thus, the breathing period is inversely proportional to the propagation constants difference between the two FB beams. Indeed, our BPM simulations verify this picture.

In order to observe these breathers, we used slab waveguide samples, onto which a waveguide array was defined by dry etching of the upper cladding. For details see Ref. [19]. In principle, the best way of achieving selective excitation of FB waves in such an array is to shape the spatial phase (and, preferably, the amplitude) of the input

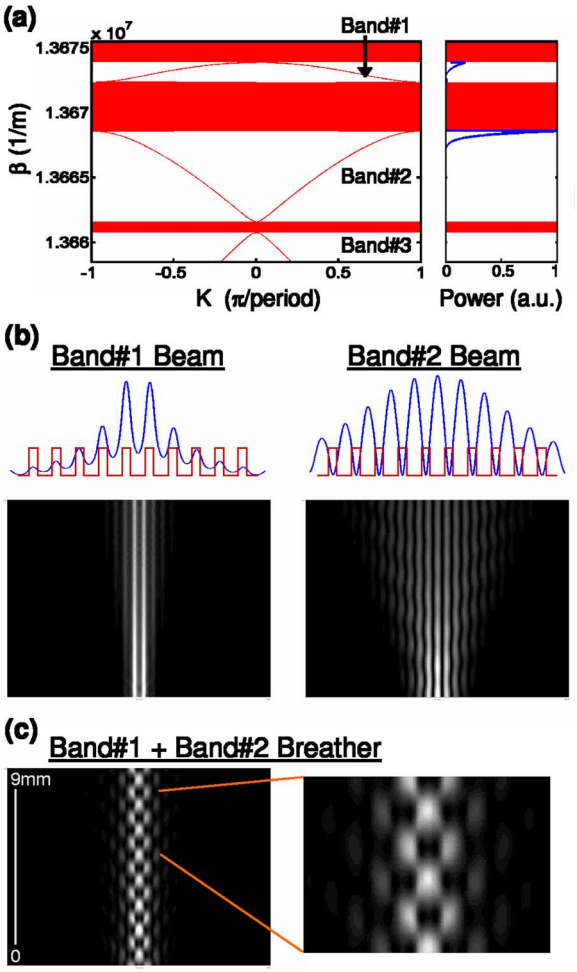

FIG. 1 (color online). BPM simulation results. (a) The band-gap diagram of the array, which relates the propagation constant (β) to the Bloch wave number (K), and the power spectrum of the two "FB beams" constituting the breather field. The shaded regions represent the gaps in the propagation constant of the FB waves. Although hardly observable in this scale, note that the diffraction curve of band No. 2 is smooth in the region of $K = 0$. (b) The two shaped FB beams are launched separately into the array at power, which is not high enough to form a soliton. Shown also are the modal shapes of the band No. 1 and band No. 2 FB waves, excited by the shaped input beams. (c) The same two beams (at the same power) are launched together into the array, jointly trapping one another and forming a breather, which propagates along the array while maintaining a constant (periodic) envelope shape. The envelope FWHM of band No. 1 and band No. 2 beam is 25 and 60 μm, respectively, and their power 300 and 700 W, respectively. The array period is 11 μm with 4 μm waveguide width and waveguide index step of 0.0015.

beam, so that it matches that of the two superimposed FB beams. In this work, however, we chose a simpler approach, in which a narrow *unshaped* Gaussian beam was launched head-on, in between a couple of neighboring array-waveguides. It has been shown recently that this configuration leads to the excitation of FB waves belonging to several bands [17], with their relative strength determined by the overlap of their modal shape with the input beam. With wide input beams (and at normal incidence), the overlap of a Gaussian beam with FB waves belonging to bands higher than band No. 1, is quite small. On the other hand, the overlap of a narrow input beam (launched between waveguides) with band No. 2 and band No. 3 FB waves may be high enough for a significant excitation of these bands.

Several waveguide-array samples were measured using this scheme, and breathers were successfully excited. Figure 2 shows typical results of such a measurement. The experimental system is similar to that used in previous experiments [19]: 120 fsec pulses emitted from a synchronously pumped optical parametric oscillator at 1.53 μm, were shaped by a cylindrical telescope, and launched head-on into the input facet of the array. The light emerging from the array was imaged onto an IR camera, and a top view of the array was imaged onto a CCD camera. We used the latter camera to monitor beam propagation in the sample, by collecting multiphoton fluorescence at the AlGaAs band gap (740 nm) excited by the high-power beam, mainly through three-photon absorption, as was verified by measuring its dependence on the input beam power. This fluorescence enables a unique view of the evolving breather along its propagation direction. Figures 2(a) and 2(c) are photographs of 11 μm-period arrays (index steps of 0.003 and 0.009,

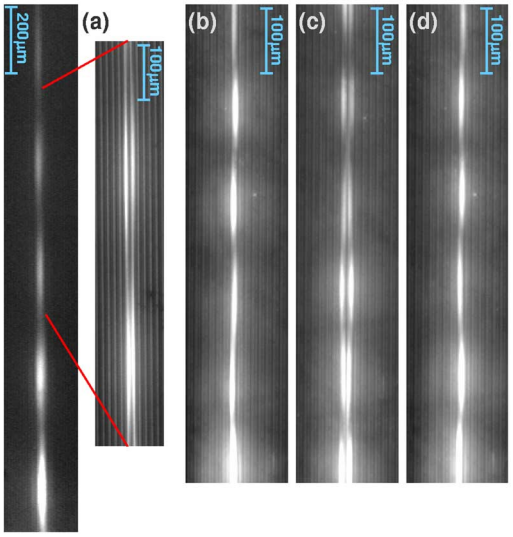

FIG. 2 (color online). Photographs of waveguide arrays, as seen from above, showing the multiphoton florescence emitted by the breathers, as they propagate along the array. Array period in all cases is 11 μm. (a) Symmetric breather in a 0.003 index-step array. (b),(d) Nonsymmetric breather, in a 0.009 index-step array. (c) Symmetric breather in the same array.

respectively), as seen from above, when a 7 μm wide beam is injected *exactly* between two neighboring waveguides. The excited breathers are clearly seen, as they propagate along the arrays. The decay of the fluorescence signal along the propagation direction is due to the dispersive temporal broadening of the laser pulse along the structure, and multiphoton absorption. The breather period remains unaffected by the decay of the pulse's peak power, since it is determined primarily by the *linear* spectrum of the system. The difference in the breathing period between Figs. 2(a)–2(c), is readily explained by the different excitation spectrum. FB-spectral analysis (described below) of the band content excited by the input beams in these two samples, reveals that in the shallow sample of Fig. 2(a), band No. 1 and band No. 2 are primarily excited, while in the deeply etched sample of Fig. 2(c), band No. 3 is also excited, leading to a faster (quasiperiodic) beating of the three bands. BPM simulations accurately confirm these findings, and, in particular, distinctive quasiperiodic breathers predicted in arrays with index-step larger than 0.0035.

We have found that the symmetric breather [as in Figs. 2(a) and 2(c)] tends to be unstable, in particular, when a significant fraction of the power is carried by band No. 1. Simulations show that such breathers, at high enough power, tend to switch into an asymmetric breather by small perturbations. This has been verified in our experiment, as seen in Figs. 2(b) and 2(d). In fact, these asymmetric breathers were much easier to excite, since any deviation from perfect symmetric launching conditions led to their excitation, while very careful alignment was needed to excite the symmetric breather of Figs. 2(a) and 2(c). The asymmetric breathers excited in this way were very stable. This behavior is readily understood, by considering the instability of the band No. 1 soliton (discrete soliton), when centered between neighboring waveguides. It has been shown that this mode of the discrete soliton is unstable, in contrast with the case in which the soliton is centered on a waveguide [20]. It is the *stable* mode of the discrete soliton, that the band No. 1 beam of the *asymmetric* breathers shown in Figs. 2(b) and 2(d), is composed of.

The beam emerging from the array was also measured, to verify that a *localized* structure is excited in the array. Typical results are shown in Fig. 3. In Fig. 3(a), cross sections of the beam at the array output are plotted as a function of the (time-average) beam power, for the case shown in Fig. 2(a). Figure 3(b) shows photographs of the beam at the array output, at low and high power. At low power, the narrow input beam excites a weakly diffracting band No. 1 beam and a strongly diffracting band No. 2 beam (discriminated by their characteristic modal shapes [17]). At high power, band No. 2 excitation is shown to narrow substantially, trapping almost completely in band No. 1 beam region, as the two beams jointly form a coherent multiband composite soliton.

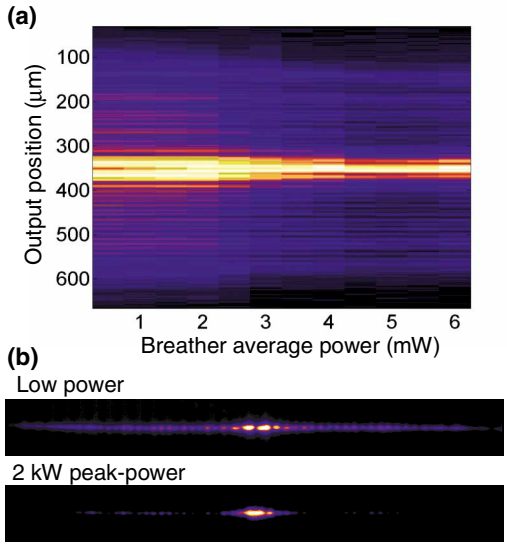

FIG. 3 (color online). Formation of the (coherent multiband composite soliton) breather shown in Fig. 2(a). (a) Cross sections of the beam at the array output as a function of the (time-average) beam power. (b) Photographs of the beam at the array output, at low and high power. At low power, the narrow input beam excites a diffracting band No. 1 and band No. 2 beams. At high power, band No. 2 excitation narrows until being trapped in band No. 1 beam region, and the breather is formed. The FWHM of the input beam was 7 μm, and the sample length was 6.4 mm.

In order to analyze the results, we performed numerical spectral analysis of the breather. Initially, BPM simulations were conducted to calculate the spatial field distribution along the sample. This field was then decomposed into the array's linear FB-waves basis, after which the spectral content of each band was summed independently to form the FB beams, i.e., the contribution from each specific band to the overall excitation. Figure 4 shows results of such an analysis. In Fig. 4(a), the power localized inside a 60 μm section of the array around the beam center, is plotted for band No. 1 and band No. 2 beams, as a function of their propagation distance along the array. At low input power, the two FB beams diffract (note the continuous drop of the central-section's power). At high power, both FB beams focus into a localized breather (characterized by a nearly constant central-section's power). Small components in band No. 3 and higher bands are also excited, but these do not seem to be trapped by the breather, and their amplitude decays as shown in Fig. 4(a). It should be noted that in all our experiment simulations, the FB beams retained a nearly constant overall power, as they propagate along the array, which suggests that the power used in our experiments was not high enough as to deform the array profile to the extent of energy transfer between bands to occur. This means that the two FB beams affect one-another solely via a mutual change of their phase front (due to the Kerr effect), while

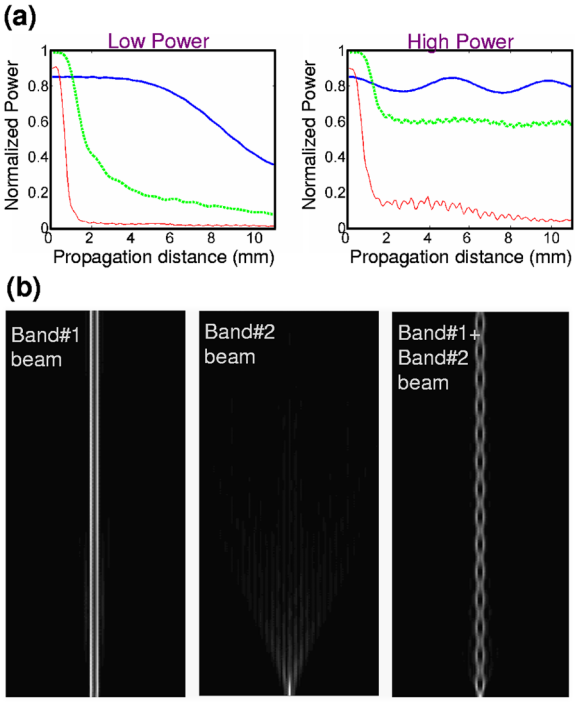

FIG. 4 (color online). Numerical analysis of the experiment. (a) The power concentrated inside a 60 μm section of the array around the beam center, normalized to the overall FB-beam power, for band No. 1 beam (thick blue line), band No. 2 beam (dashed green line), and band No. 3 beam (thin red line), plotted as a function of their propagation distance along the array, for low and high input power. (b) Top view of simulation of band No. 1 beam and band No. 2 beam, when launched separately and together into the array at the same high power level as in the right panel of (a). The band No. 2 beam is trapped by the band No. 1 beam, to form a breather, while a small band No. 3 component diffracts even at high input powers.

almost no energy is transferred between them. Figure 4(b) shows simulations of the high-power beam propagation, when each of the FB beams excited by the input beam are sent separately, and then together into the sample. Band No. 1 beam, launched *separately* into the array, formed a discrete soliton, centered between a couple of waveguides, having a width of about 1.5 array-periods. Band No. 2 beam, launched *separately* into the array, diffracted into a very wide output. Band No. 1 and band No. 2 beams, launched *together* into the array, excited a breather, as shown in the right panel of Fig. 4(b). This proves that for this breather, band No. 2 beam is trapped by band No. 1 beam (but not the other way around), in analogy with noncoherent composite solitons.

In conclusion, we have reported the observation of multiband FB breathers in nonlinear waveguide arrays. This system enables direct observation of their internal dynamics due to multiphoton fluorescence generated in our AlGaAs waveguides. The FB approach was shown to be useful to address issues such as their structure, stability, and dynamics.

The authors gratefully acknowledge Oren Cohen from the Physics Department in the Technion Israel Institute of Technology for valuable and useful discussions, and the BSF (Binational Science Foundation) and the German-Israeli Project Cooperation (DIP) for financial support.

*Electronic address: daniel.mandelik@weizmann.ac.il
†Currently at the Physics Department, University of California Santa Barbara, Santa Barbara, CA 93106, USA.
‡Currently at Université du Quebec, Institute national de la recherche scientifique, Varennes, Quebec, Canada J3X 1S2.

[1] R. S. MacKay and S. Aubry, Nonlinearity **7**, 1623 (1994); see also S. Aubry, Physica (Amsterdam) **103D**, 201 (1997).
[2] S. Flach and C. R. Willis, Phys. Rep. **295**, 181 (1998); O. M. Braun and Yu. S. Kivshar, *ibid.* **306**, 1 (1998), Sec. 6.
[3] R. S. MacKay and J.-A. Sepulchre, Physica (Amsterdam) **119D**, 148 (1998).
[4] B. I. Swanson, J. A. Brozik, S. P. Love, G. F. Strouse, A. P. Shreve, A. R. Bishop, W. Z. Wang, and M. I. Salkola, Phys. Rev. Lett. **82**, 3288 (1999).
[5] F. M. Russell, Y. Zolotaryuk, J. C. Eilbeck, and T. Dauxois, Phys. Rev. B **55**, 6304 (1997).
[6] R. Lai and A. J. Sievers, Phys. Rep. **314**, 147 (1999).
[7] U. T. Schwarz, L. Q. English, and A. J. Sievers, Phys. Rev. Lett. **83**, 223 (1999).
[8] E. Trias, J. J. Mazo, and T. P. Orlando, Phys. Rev. Lett. **84**, 741 (2000).
[9] P. Binder, D. Abraimov, A. V. Ustinov, S. Flach, and Y. Zolotaryuk, Phys. Rev. Lett. **84**, 745 (2000).
[10] M. Peyrard and J. Farago, Physica (Amsterdam) **288A**, 199 (2000).
[11] A. Trombettoni and A. Smerzi, Phys. Rev. Lett. **86**, 2353 (2001).
[12] J. N. Kutz and S. G. Evangelides, Jr., Opt. Lett. **23**, 685 (1998).
[13] S. F. Mingaleev, Yu. S. Kivshar, and R. A. Sammut, Phys. Rev. E **62**, 5777 (2000).
[14] M. Mitchell, M. Segev, and D. Christodoulides, Phys. Rev. Lett. **80**, 4657 (1998).
[15] A. S. Desyatnikov, D. Neshev, E. A. Ostrovskaya, Yu. S. Kivshar, G. McCarthy, W. Krolikowski, and B. Luther-Davies, J. Opt. Soc. Am. B **19**, 586 (2002).
[16] O. Cohen, T. Schwartz, J. W. Fleischer, M. Segev, and D. N. Christodoulides, Technical Digest of the CLEO Conference, QMC7, Baltimore, Maryland, USA, 2003.
[17] D. Mandelik, H. S. Eisenberg, Y. Silberberg, R. Morandotti, and J. S. Aitchison, Phys. Rev. Lett. **90**, 053902 (2003).
[18] The BPM code is available at www.FreeBPM.com
[19] H. S. Eisenberg, Y. Silberberg, R. Morandotti, A. R. Boyd, and J. S. Aitchison, Phys. Rev. Lett. **81**, 3383 (1998).
[20] W. Krolikowsky and Yu. S. Kivshar, J. Opt. Soc. Am. B **13**, 876 (1996).